Pramāṇa, Vol. 21, No. 2, August 1983, pp. 131–148. © Printed in India.

Analytical studies of gain optimization in CO_2-N_2 gasdynamic lasers employing two-dimensional wedge nozzles

V SHANMUGASUNDARAM* and N M REDDY
Department of Aerospace Engineering,
Indian Institute of Science, Bangalore 560 012, India
*Now at University of Edinburgh, England

MS received 12 January 1983; revised 4 June 1983

Abstract. An analytical method has been proposed to optimise the small-signal-optical gain of CO_2–N_2 gasdynamic lasers (GDL) employing two-dimensional (2D) wedge nozzles. Following our earlier work the equations governing the steady, inviscid, quasi-one-dimensional flow in the wedge nozzle of the GDL are reduced to a universal form so that their solutions depend on a single unifying parameter. These equations are solved numerically to obtain similar solutions for the various flow quantities, which variables are subsequently used to optimize the small-signal-gain. The corresponding optimum values like reservoir pressure and temperature and 2D nozzle area ratio also have been predicted and graphed for a wide range of laser gas compositions, with either H_2O or He as the catalyst. A large number of graphs are presented which may be used to obtain the optimum values of small signal gain for a wide range of laser compositions without further computations.

Keywords. Gasdynamic laser; population inversion; small signal gain; area ratio; wedge nozzle.

1. Introduction

In recent times a great deal of effort has gone into the study of small-signal optical-gain performance of CO_2-N_2 gasdynamic laser (GDL) system (see Christiansen *et al* 1975 and Anderson 1976 for extensive surveys on the literature). The emphasis has been to study (to a limited extent) the influence of either one of the parameters like reservoir conditions, gas mixture composition etc., on the performance characteristics of these devices. Even the recent analytical optimization study for the small-signal gain in 2D wedge nozzles by Losev and Makarov (1975) and the closed form engineering correlation for the peak small-signal gain by McManus and Anderson (1976) were only limited in their approach in the sense that they were restricted to either a prescribed nozzle configuration, reservoir condition or gas composition; they did not propose any generalized approach which would yield some universal correlating parameter (combining all of the GDL parameters). In an attempt to overcome this deficiency, the present authors have developed a completely generalized characterization of the GDL performance in a formal way and have identified the general correlating parameters controlling the GDL performance; these correlating parameters were then used to optimize the small-signal gain on a pre-selected vibrational-rotational transition and subsequently obtained the combination of operating parameters that would yield such optimum gain values (Reddy and Shanmugasundaram 1979a).

Detailed results from such an optimization study of the small-signal gain in CO_2-N_2 GDL on the P(20) 001 → 100 vibrational-rotational transition have been presented for families of conical and hyperbolic nozzles (Reddy and Shanmugasundaram 1979b), with H_2O and He as catalysts. Some preliminary results for two-dimensional (2D) wedge nozzle-flows, with He as catalyst were also presented at the second International Symposium on Gas flow and Chemical Lasers (Reddy and Shanmugasundaram 1978). The present paper presents the complete optimization results in detail for 2D wedge nozzles, with either He (to be called system 1) or H_2O (to be called system 2) as catalyst. Further, unlike as in Reddy and Shanmugasundaram (1979a, b), where the nozzle-flow solutions have been presented only for the region downstream of the nozzle throat, here the solutions are obtained starting right from the nozzle reservoir. This way, any possible non-equilibrium condition in the flow upstream of the nozzle throat (Anderson 1969, 1970) is treated in the calculations.

The analysis in the present paper is based on the method given by Reddy and Shanmugasundaram (1979a), according to which the system of equations governing the steady, inviscid, quasi-one-dimensional, non-reacting flow of a mixture of gases in vibrational non-equilibrium in a GDL nozzle reduced to a universal form so that the solutions depend on a single correlating parameter χ_I, which combines all the other operating parameters of the problem. In this paper we shall present the numerical results from the parametric study of these equations for a particular family of nozzle shapes, *viz* 2D wedge, and discuss how these solutions can be used to optimize the small-signal-optical-gain coefficient G_0 for the P(20) 001→100 vibrational-rotational transition. We shall also discuss a method of obtaining the combination of optimum operating conditions like reservoir quantities and nozzle shape, which would yield the optimum value of small signal gain.

2. Governing equations

For the two-temperature vibrational model (see Anderson 1976 for details and figure 1 for the schematic) employed here, the governing equations to be considered are the three global conservation equations, the equation of state and the two rate equations governing the relaxation of the two vibrational modes, of temperatures T_I' and T_{II}'

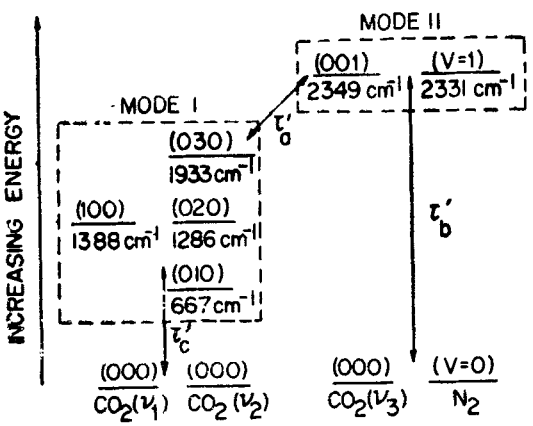

Figure 1. Schematic of the vibrational model (Anderson 1976).

respectively. Two more algebraic equations give the population inversion (PI) and the small-signal-optical-gain as functions of the flow quantities obtained from the afore-mentioned governing equations. The publications of Anderson (1976) and Losev and Makarov (1975) give complete details of these equations in their dimensional forms. The details of how these equations are normalized and then reduced to a universal form so that their solutions depend on a single parameter, which combines all the other parameters of the problem are given by Reddy and Shanmugasundaram (1979a). Here, we only reproduce the necessary equations in their final normalized forms, retaining the same nomenclature as in the above reference.

The generalized momentum equation, obtained by combining the momentum and energy equations, and the equation of state, is

$$\psi - \alpha \frac{d\psi}{d\xi} - X_C \sum_{m = I, II} \bar{G}_m \frac{d\phi_m}{d\xi} = 0. \tag{1}$$

The rate equation (of the Landu-Teller type), governing the relaxation of the vibrational energy of mode m (m=I, II), is

$$\frac{d\phi_m}{d\xi} = \frac{K_m \psi}{N_s} \exp\left[\chi_m + \xi\,(1 - 1/ij) - \gamma_{ll}\,\psi^{-1/3}\right] \cdot \left[\frac{\bar{E}_e - \bar{E}}{\bar{G}}\right]_m. \tag{2}$$

In (2) the subscript e refers to local equilibrium value and l=C for m=I and l=N for m=II, where C and N denote respectively CO_2 and N_2.

In this analysis the P(20) transitions at a wavelength of 10·6 μm and occurring between J=19 rotational level of 001 and J=20 rotational level of 100 vibrational levels of CO_2 are considered. Further, only the optical line broadening mechanism in its Lorentz (homogeneous) limit is considered. Accordingly, the equations for the population inversion and small-signal gain are:

$$\mathrm{PI} = \frac{\exp\left(-\bar{\theta}_{\nu_3}/\phi_{II}\right) - \exp\left(-\bar{\theta}_{\nu_1}/\phi_I\right)}{\bar{Q}_{\mathrm{vib}}}, \tag{3}$$

and

$$G_0/m = 9{\cdot}77\,\frac{(\mathrm{PI})}{P(X_l)\,\psi^{3/2}} \exp\left(-0{\cdot}0703/\psi\right), \tag{4}$$

where,

$$\bar{Q}_{\mathrm{vib}} = \left[1 - \exp\left(-\bar{\theta}_{\nu_1}/\phi_I\right)\right]^{-1} \left[1 - \exp\left(-\bar{\theta}_{\nu_2}/\phi_I\right)\right]^{-2} \times \left[1 - \exp\left(-\bar{\theta}_{\nu_3}/\phi_{II}\right)\right]^{-1} \tag{5}$$

and

$$P(X_l) = 1 + 0{\cdot}7589\,(X_N/X_C) + b\,(X_H/X_C), \tag{6}$$

with b = 0·3836 for H_2O and b = 0·6972 for He catalyst.

In the above equations, X_C, X_N and X_H are respectively the mole fractions of CO_2, N_2 and the catalyst H_2O or He. In equation (1), $\alpha = [2{\cdot}5\,(X_C + X_N) + 0{\cdot}5n\,X_H]$, where n is the number of degrees of freedom of the catalyst. The parameters i and j

govern the shape of the nozzle; for example $i = 1$ and $j = 1$ for wedge nozzles. The normalized temperature $\psi = T'/\theta'_{\nu_N}$ and the vibrational temperatures for modes I and II, $\phi_m = T'_m/\theta'_{\nu_N}$, $m = \text{I, II}$, are normalized with respect to θ'_{ν_N} (= 3357°K), the characteristic temperature for the normal vibrational mode of N_2, where the primes denote dimensional quantities. The normalized characteristic temperatures for the three vibrational modes of CO_2 are defined as $\bar{\theta}_{\nu_n} = \theta'_{\nu_n}/\theta'_{\nu_N}$, $n = 1, 2, 3$ ($\theta'_{\nu_1} = 1999°K$; $\theta'_{\nu_2} = 960°K$; $\theta'_{\nu_3} = 3373°K$).

The independent variable ξ is defined as,

$$\xi = S_0 + \ln \rho = S_0 - \ln [(u/u_*)(A/\rho_*)], \tag{7}$$

where $\rho = \rho'/\rho'_0$ is the normalized density in which the suffix 0 refers to reservoir conditions, and S_0 is the specific entropy given by

$$S_0 = -\ln \rho_e + \alpha \ln \psi_e + \frac{X_C}{\psi_e}[\bar{E}_{\text{I}} + \bar{E}_{\text{II}}]_e - X_C \ln \{[1 - \exp(-\bar{\theta}_{\nu_1}/\psi)] \times [1 - \exp(-\bar{\theta}_{\nu_2}/\psi)]^2 [1 - \exp(-\bar{\theta}_{\nu_3}/\psi)] \times \cdot [1 - \exp(-1/\psi)]^{X_N/X_C}\}_e + S_r, \tag{8}$$

where S_r is a reference value of S_0 and for the wedge nozzles $S_r = 26{\cdot}29$ for He catalyst and $S_y = 29{\cdot}57$ for H_2O catalyst.

The various functions occurring in the above equations are defined as

$$\bar{E}_{\text{I}} = \frac{\bar{\theta}_{\nu_1}}{\exp(-\bar{\theta}_{\nu_1}/\phi_{\text{I}}) - 1} + \frac{2\bar{\theta}_{\nu_2}}{\exp(-\bar{\theta}_{\nu_2}/\phi_{\text{I}}) - 1}, \tag{9}$$

$$\bar{E}_{\text{II}} = \frac{\bar{\theta}_{\nu_3}}{\exp(\bar{\theta}_{\nu_3}/\phi_{\text{II}}) - 1} + \frac{X_N/X_C}{\exp(1/\phi_{\text{II}}) - 1}, \tag{10}$$

$$\bar{G}_{\text{I}} = \left(\frac{\bar{\theta}_{\nu_1}}{\phi_{\text{I}}}\right)^2 \frac{\exp(\bar{\theta}_{\nu_1}/\phi_{\text{I}})}{[\exp(\bar{\theta}_{\nu_1}/\phi_{\text{I}}) - 1]^2} + 2\left(\frac{\bar{\theta}_{\nu_2}}{\phi_{\text{I}}}\right)^2 \frac{\exp(\bar{\theta}_{\nu_2}/\phi_{\text{I}})}{[\exp(\bar{\theta}_{\nu_2}/\phi_{\text{I}}) - 1]^2}, \tag{11}$$

$$\bar{G}_{\text{II}} = \left(\frac{\bar{\theta}_{\nu_3}}{\phi_{\text{II}}}\right)^2 \frac{\exp(\bar{\theta}_{\nu_3}/\phi_{\text{II}})}{[\exp(\bar{\theta}_{\nu_3}/\phi_{\text{II}}) - 1]^2} + \frac{X_N}{X_C}\left(\frac{1}{\phi_{\text{II}}^2}\right) \frac{\exp(1/\phi_{\text{II}})}{[\exp(1/\phi_{\text{II}}) - 1]^2}, \tag{12}$$

$$K_{\text{I}} = X_C + X_N [(\tau'_c)_{CC}/(\tau'_c)_{CN}] + X_H [(\tau'_c)_{CC}/(\tau'_c)_{CH}], \tag{13}$$

$$K_{\text{II}} = [X_C K_a (\tau'_b)_{NN}/(\tau'_a)_{CC} + X_N K_b]/(X_C + X_N), \tag{14}$$

where $$K_a = X_C + X_N\,[(\tau'_a)_{CC}/(\tau'_a)_{CN}] + X_H\,[(\tau'_a)_{CC}/(\tau'_a)_{CH}], \tag{15}$$

and $$K_b = X_C\,[(\tau'_b)_{NN}/(\tau'_b)_{NC}] + X_N + X_H\,[(\tau'_b)_{NN}/(\tau'_b)_{NH}]. \tag{16}$$

In (13) to (16), τ's are the vibrational relaxation times for various collisional partners.

The parameters χ_m used in (2) are defined, in general, as

$$\chi_m = \ln\left(\frac{P'_0\,L'\,\theta'_{\nu_N}\,(\rho_* u_*)^{a+1/ij}}{ij\,R'^{1/2}_m\,T'^{3/2}_0\,J_{ll}}\right) - (1 - 1/ij)\,S_0, \quad m = \text{I, II} \tag{17}$$

where p'_0 is the reservoir pressure, T'_0 is the resevoir temperature, R'_m is the mixture gas constant, ρ_* and u_* are the normalized density and velocity at the throat and L' is the nozzle shape parameter. The values of the constants γ's and J's occurring in (2) and (17) are

$$\gamma_{CC} = 2{\cdot}7389; \qquad J_{CC} = 1{\cdot}555 \times 10^{-8} \text{ atm-sec.}$$

$$\gamma_{NN} = 14{\cdot}3098; \quad J_{NN} = 2{\cdot}450 \times 10^{-11} \text{ atm-sec.} \tag{18}$$

The parameters χ for the case of wedge nozzles is obtained by substituting $ij = 1$ and $a = 7{\cdot}2$ for He catalyst and $a = 8{\cdot}82$ for H_2O catalyst in (17).

The details of the derivation of these governing equations are given in Reddy and Shanmugasundaram (1979a).

The quantity N_s occurring in (2), for any given ij, is a function of local velocity, Mach number and area ratio and hence is indirectly dependent on the reservoir conditions. The computer program of Lordi *et al* (1966) is used to compute the function N_s. Since it was found that the variation of N_s with reservoir pressure very small we have assumed a constant reservoir pressure $p'_0 = 10$ atm. The N_s is computed for the reservoir temperatures, $T'_0 = 1000$, 1500, 2000 and 3000°K, for a wide range of mixture compositions. These values of N_s are plotted as a function of (ξ_*/ξ), where ξ_* is the value of independent variable ξ at the nozzle throat, for each composition at different reservoir temperatures. Then the different values of N_s for each (ξ_*/ξ) are tabulated with the help of above graphs. The final average correlation for N_s is computed from these tabulated values and plotted as a function of (ξ_*/ξ). Figure 2 shows these average N_s correlations for systems 1 and 2.

In the case of wedge nozzles, the N_s correlations for both the systems are represented (obtained by curve fitting) by the following simple analytical expressions:

$$N_s = 0 \text{ for } \xi_*/\xi \leqslant 0{\cdot}985$$

$$= 0{\cdot}088 - 0{\cdot}682\,(0{\cdot}995 - \xi_*/\xi)^{0{\cdot}45}, \text{ for } 0{\cdot}985 < \xi_*/\xi \leqslant 0{\cdot}995$$

$$= 0{\cdot}436 - 8{\cdot}6 \times 10^{-3}\,(\xi_*/\xi - 0{\cdot}85)^{-1{\cdot}9} \text{ for } \xi_*/\xi > 0{\cdot}995, \tag{19}$$

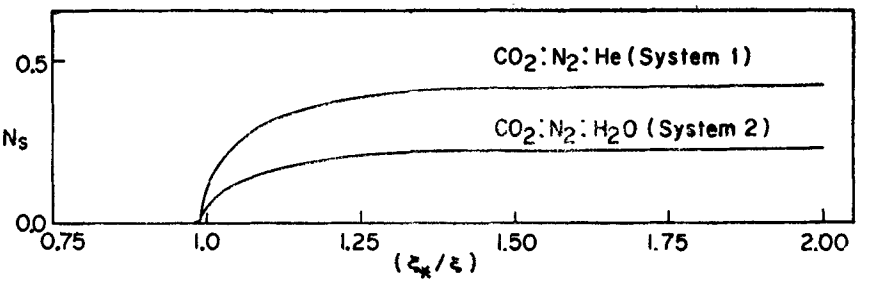

Figure 2. Correlation of function N_s with the parameter (ξ_*/ξ) for systems 1 and 2.

for system 1 and

$$N_s = 0 \text{ for } \xi_*/\xi \leqslant 0{\cdot}985$$

$$= 0{\cdot}039 - 0{\cdot}118\,(0{\cdot}995 - \xi_*/\xi)^{0{\cdot}241}, \text{ for } 0{\cdot}985 < \xi_*/\xi \leqslant 0{\cdot}995$$

$$= 0{\cdot}233 - 4{\cdot}410 \times 10^{-3}\,(\xi_*/\xi - 0{\cdot}816)^{-02{\cdot}186} \text{ for } \xi_*/\xi > 0{\cdot}995, \qquad (20)$$

for system 2.

Similarly the mass flow factor, $\rho_* u_*$ and the nozzle throat density ρ_* have also been correlated as functions of only the reservoir temperature in the case of wedge nozzles and are given by the following expressions.

For He catalyst:

$$\rho_* u_* = k_1 = 0{\cdot}686 - 8{\cdot}0 \times 10^{-8}\, T_0' \,(^\circ\text{K});$$

$$\rho_* = k_2 = \text{constant} = 0{\cdot}63. \qquad (21)$$

For H_2O catalyst:

$$\rho_* u_* = k_1 = \text{constant} = 0{\cdot}66;$$

$$\rho_* = k_2 = \text{constant} = 0{\cdot}63. \qquad (22)$$

Variations in the normalized velocity ratio (u/u_*) along the nozzle are also influenced significantly by the reservoir conditions (see Reddy and Shanmugasundaram 1978 for detailed results). Again, using the computer program of Lordi *et al* (1966) u/u_* has been correlated as a function of only the normalized area, $A = A'/A'_* = [1 + (x'/L')^j]^i$ (where $i = j = 1$ for wedge nozzles and x' is the distance in the flow direction), and is given by

For He catalyst:

$$k_1^{3{\cdot}37}\,(u/u_*) = [-0{\cdot}022 + 0{\cdot}049\,(0{\cdot}3 + \log_{10} A)^{-1{\cdot}5}] \text{ for } M < 1,$$

$$= [1{\cdot}165 - 0{\cdot}560\,(0{\cdot}1 + \log_{10} A)^{-0{\cdot}2}] \text{ for } M \geqslant 1; \qquad (23)$$

For H_2Ocatalyst:

$$k_1^{3.98}(u/u_*) = [-0.0217 + 0.0399\,(0.234 + \log_{10} A)^{-1.197}] \text{ for } M < 1,$$

$$= [0.669 - 0.216\,(0.194 + \log_{10} A)^{-0.467}] \text{ for } M \geqslant 1. \quad (24)$$

Here M is the Mach number. These correlations have been presented in figure 3.

The analytical expressions given in equations (19) to (24) for the correlations are obtained by curve fitting.

Since PI and G_0, as given by the algebraic equations (3) and (4), are only functions of the gas composition, and ϕ_I, ϕ_{II} and ψ, the emphasis here would be on obtaining the solutions for the last three variables. The differential equations (1) and (2) governing these three variables reveal that for a given gas mixture and value of ij, the solutions of these equations as a function of ξ depend on only one parameter χ_I, which combines, as can be seen from (17), all the other parameters of the problem, like p_0', T_0', L' etc. In this sense, the solutions obtained thus will be 'universal'.

3. Results and discussion

For any given laser mixture, (1) and (2) are solved simultaneously for the three unknowns ϕ_I, ϕ_{II} and ψ, with χ_I as the parameter. The numerical integration is carried out using the modified, fourth order *R-K-G* method. Since the flow in a GDL starts from a reservoir, wherein the hot gas mixture is in vibrational equilibrium, the initial values for the three temperatures correspond to this equilibrium state. To obtain the numerical solutions starting from the reservoir, the procedure is as follows: since (21) or (22) (corresponding to system 1 or 2) gives the value of ρ_*, ξ_* is estimated from (7)

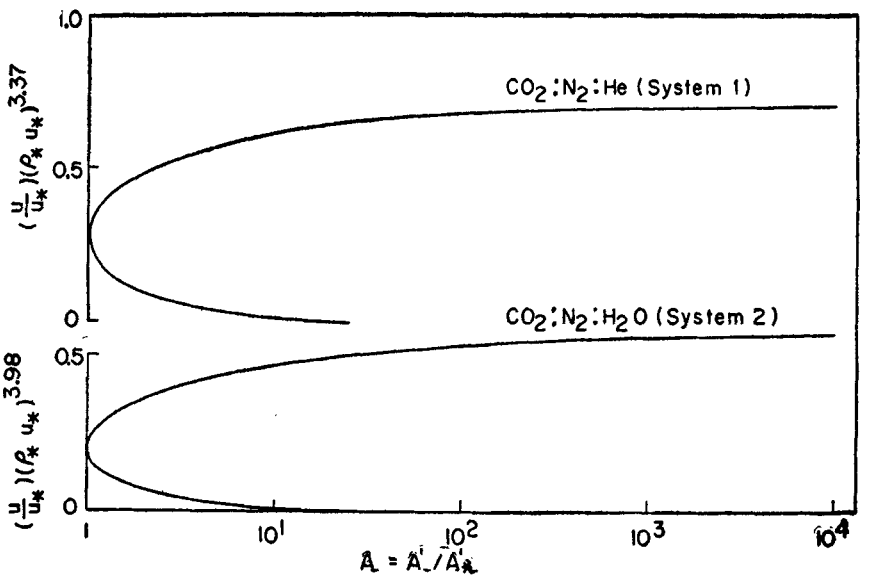

Figure 3. Correlation of velocity ratio (u/u_*) with area ratio for systems 1 and 2.

with known S_0 from the reservoir conditions. At every point along the nozzle, *i.e.* for every value of ξ (with ξ decreasing in the flow direction), ξ/ξ_* and the corresponding value of N_s from either (19) or (20) are calculated depending on whether it is system 1 or 2. If $N_s=0$, which means the flow is in local vibrational equilibrium (see (2)), the corresponding equilibrium solution is obtained using the method given by Reddy and Shanmugasundaram (1979a). For any other value of $N_s > 0$, implying the prevalence of non-equilibrium conditions within the nozzle, we solve the differential equations (1) and (2) for the three unknowns ϕ_I, ϕ_{II} and ψ; the appropriate initital values would correspond to the ψ_e value obtained at the last st:p of the local equilibrium calculations. Knowing the temperature distributions along the nozzle, PI and G_0 as functions of ξ are calculated from (3) and (4).

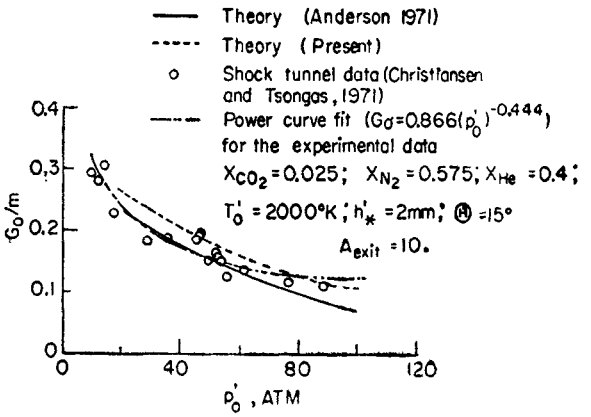

Figure 4. Variation of small-signal gain at the exit of a 2D wedge nozzle with reservoir pressure; comparison with existing results (Christiansen and Tsonges 1971; Anderson 1971).

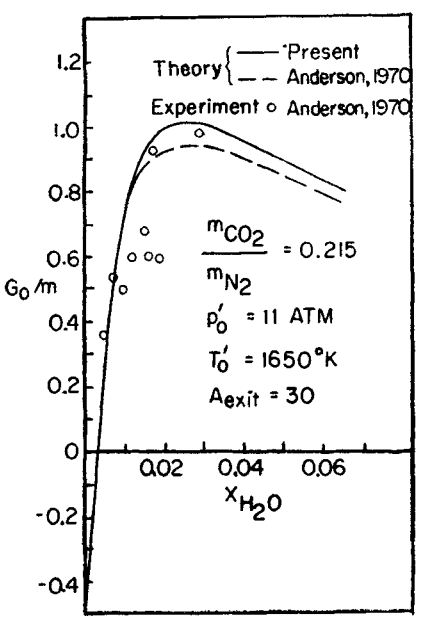

Figure 5. Variation of small-signal gain at the exit of a 2D wedge nozzle with H_2O content; comparison with existing results (Anderson 1970).

Figures 4 and 5 show values of G_0 at the exit of a wedge nozzle, obtained by the present method, for systems 1 and 2 respectively; for the exit area ratios of 10 and 30 considered here, values of L' are respectively 0·3732 cm and 0·1486 cm. The relevant operating conditions, also contained in the figures, have been taken from Anderson (1969, 1970) and Anderson *et al* (1971). For these conditions, first we estimate ξ_0 and X_I from (7) and (17) and obtain the numerical solutions as described earlier. Figures 4 and 5 also contain results from experiments (Anderson 1970 and Christiansen and Tsonges 1971) as well as from Anderson's time-dependent analysis (Anderson 1970, Anderson *et al* 1971). The difference between the experiments and Anderson's theory is believed to be due to many uncertain factors like: (i) the errors involved in the estimation of vibration relaxation rates, (ii) use of simplified two-mode vibrational model and (iii) measurement errors which have not been discussed by Christiansen and Tsonges (1971). The difference between the theoretical values obtained by Anderson and the present computations is believed to be due to use of correlated values for N_s, $\rho_* u_*$ and ρ_* in the present analysis.

Computations are first carried out for a wide range of mixture compositions for both systems 1 and 2; Table 1 contains the details of the mixture compositions considered. Figures 6 and 7 show typical solutions for two sample cases, one each for the two systems. An interesting aspect of these solutions is the tendency of G_0 to attain a maximum while PI tends to remain constant far downstream of the nozzle throat and the reasons for such behaviour have been discussed in detail by Reddy and Shanmugasundaram (1979a).

Table 1. Values of N_2 mole-fraction

System 1

X_{He}	X_{CO_2}						
	0·025	0·05	0·075	0.1	0·15	0·2	0·25
0·2	0·775	0·75	0·725	0·7	0·65	0·6	0·55
0·3	0·675	0·65	0·625	0·6	0·55	0·5	0·45
0·4	0·575	0·55	0·525	0·5	0·45	0·4	0·35
0·5	0·475	0·45	0·425	0·4	0·35	0·3	0·25
0·6	0·375	0·35	0·325	0·3	0·25	0·2	0·15

System 2

X_{CO_2}	X_{H_2O}							
	0·01	0·02	0·04	0·06	0·08	0·1	0·15	0·2
0·050	0·94	0·93	0·91	0·89	0·87	0·85	0·80	0·75
0·075	0·915	0·905	0·885	0·865	0·845	0·825	0·775	0·725
0·10	0·89	0·88	0·86	0·84	0·82	0·80	0·75	0·70
0·15	0·84	0·83	0·81	0.79	0·77	0.75	0·70	0·65
0·20	0·79	0·78	0·76	0·74	0·72	0·70	0·65	60·0
0·25	0·74	0·73	0·71	0.69	0·67	0·65	0·60	0·55
0·30	0·69	0·68	0·66	0·64	0·62	0·60	0·55	0·50

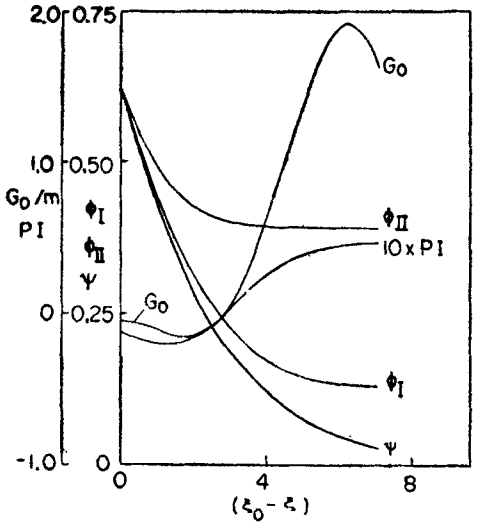

Figure 6. Variation of flow quantities along the GDL nozzle for $X_{CO_2} = 0{\cdot}15$; $X_{N_2} = 0{\cdot}35$; $X_{He} = 0{\cdot}5$; $ij = 1$; $\chi_I = 4{\cdot}5$; $\psi_0 = 0{\cdot}625$; $\xi_0 = 26{\cdot}36$.

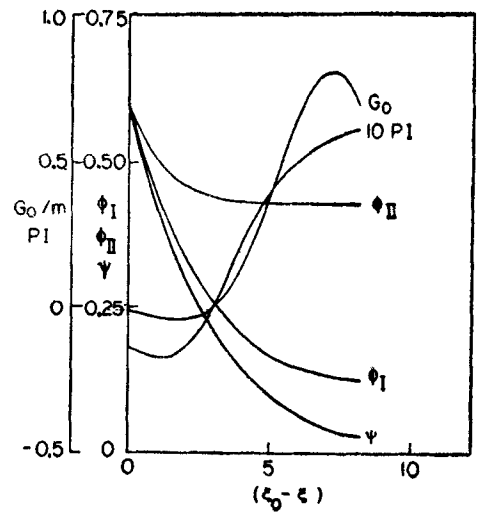

Figure 7. Variation of flow quantities along the GDL nozzle for $X_{CO_2} = 0{\cdot}05$; $X_{N_2} = 0{\cdot}94$; $X_{H_2O} = 0{\cdot}01$; $ij = 1$; $\chi_I = 4{\cdot}48$; $\psi_0 = 0{\cdot}601$; $\xi_0 = 29{\cdot}115$.

For each gas composition, such peak values of G_0 are obtained for a wide range of values of χ_I (with ψ_0 chosen appropriately in each case), and are plotted in figures 8 and 9 for systems 1 and 2 respectively. From these figures it is apparent that G_0 attains a maximum value at a particular value of χ_I for every gas composition and these two quantities are designated respectively as $(G_0)_{optimum}$ and $(\chi_I)_{optimum}$. Thus, for a given laser mixture, $(G_0)_{opt}$ represents the highest possible value of small-signal optical gain coefficient on the $P(20)$ transition at 10·6 μm. Larger gain coefficients could exist on other 001→100 vibrational-rotational transitions. The present analysis could be easily extended to calculate the maximum gain over the entire set of

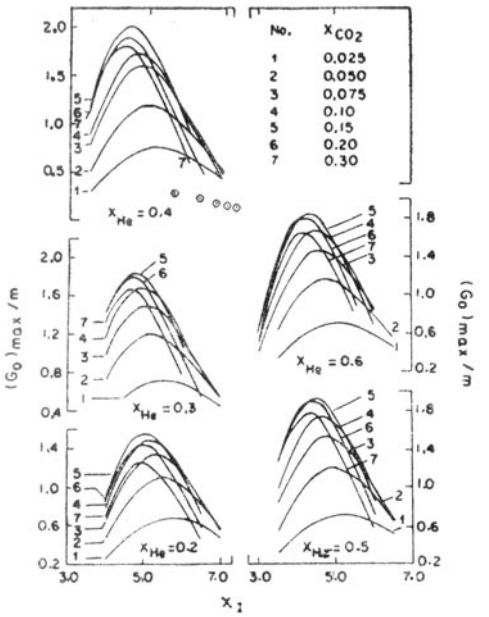

Figure 8. Variation of maximum values of small-signal gain on the P(20) 001→100 transition with χ_1 for various mixture compositions in system 1.

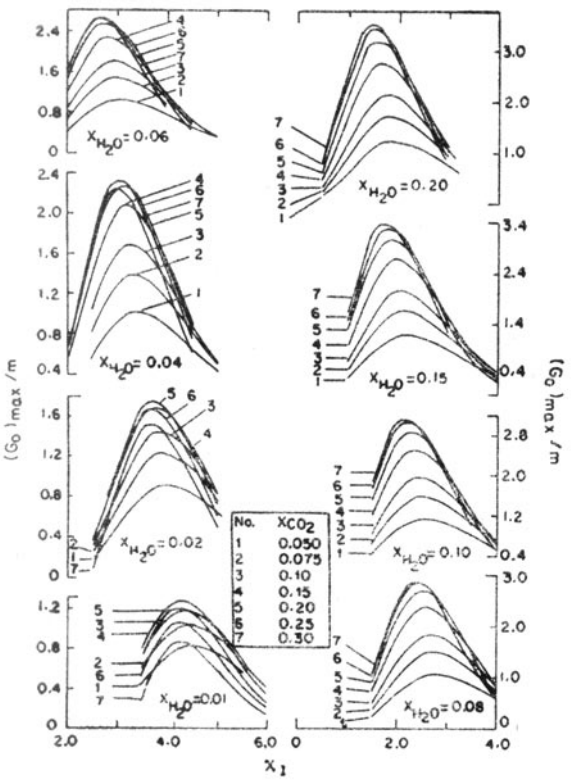

Figure 9. Variation of maximum values of small-signal-gain on the P(20) 001→100 transition with χ_1 for various mixture compositions in system 2.

allowed P-branch transitions; however, that theoretical development is not presented here.

For system 1, experimental results presented in figure 4 for the G_0 values at the exit of a 2D wedge nozzle have also been replotted in figure 8 for comparison. It can be easily seen that these values differ significantly from the maximum gain values possible for the same gas composition of 2·5% CO_2, 57·5% of N_2 and 40% He, as obtained by the present method. This deviation is attributable to the nozzle area ratio of 10 employed for obtaining experimental data shown in figure 4 being less than optimum for the operating conditions developed; in other words, for the experimental nozzle,

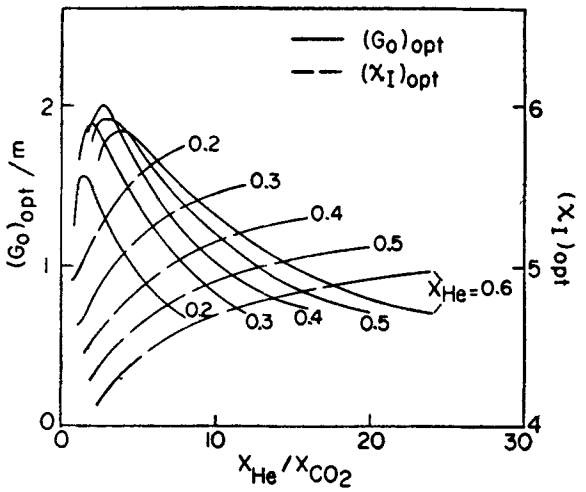

Figure 10. Effect of ratio of mole-fractions of He and CO_2 on optimum values of χ_I and small-signal-gain on the P(20) 001→100 transition.

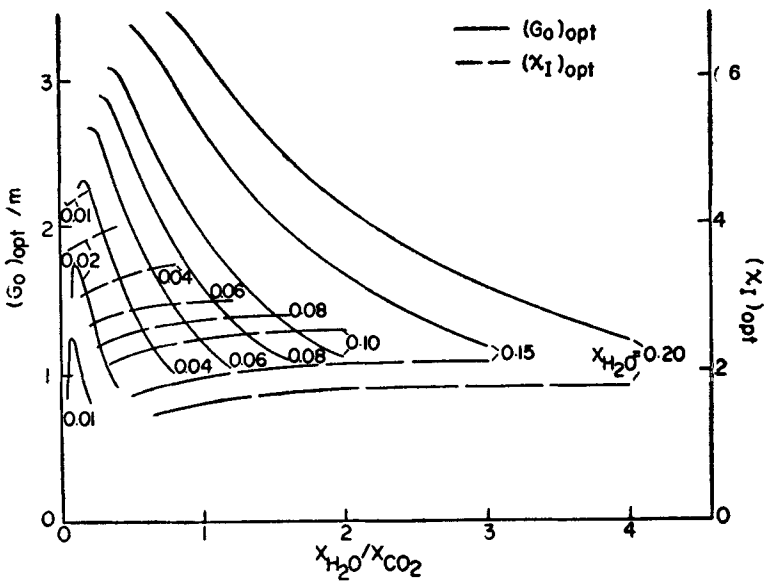

Figure 11. Effect of ratio of mole-fractions of H_2O and CO_2 on optimum values of χ_I and small-signal-gain on the P(20) 001→100 transition.

the GDL gas is only partially expanded as it approaches the exit, which results in much smaller values for the small-signal gain. Therefore, it can be inferred that by employing much larger expansion ratios than that given in figure 4, one would have obtained much higher values for G_0 for the same operating conditions. These observations are also true for the experimental results presented in figure 5 for H_2O catalyst.

To study the influence of CO_2 and catalyst concentration on the optimum value of G_0, these quantities have been cross-plotted in figures 10 and 11 as a function of the ratio of mole-fractions of the catalyst and CO_2. An inspection of these figures reveal that, for a given catalyst mole-fraction, $(G_0)_{opt}$ attains a maximum at some value of the CO_2 mole-fraction, which may be due to a combination of factors like (i) the decrease in the N_2 content because of the increase in the mole-fraction of CO_2, with a consequent adverse effect on the 'pumping reaction' which is essential for populating the upper laser level and (ii) the effectiveness of increasing concentration of the CO_2 molecules itself in the collisional de-activation of the upper laser level. This value of CO_2 at which $(G_0)_{opt}$ peaks out increases with increasing catalyst content. Figures 10 and 11 also show the tendency of $(G_0)_{opt}$ to peak around 40 mole-% of He in system 1 and around 20 mole-% of H_2O in system 2. The reason for such a trend in $(G_0)_{opt}$ is that as the catalyst number density increases, besides the lower laser level which is rapidly de-excited by the catalyst, the upper laser level population also is affected adversely with a consequence that the PI and hence G_0 are reduced. From the foregoing observations it may be concluded that small-signal optical-gains as high as $2/m$ in system 1 and $3{\cdot}5/m$ in system 2 are possible and that such high values can be obtained by employing laser mixtures containing CO_2 and He mole-fractions of 15% and 40% respectively in system 1 or CO_2 and H_2O mole-fractions of 30% and 20% respectively in system 2. Figures 10 and 11 also depict the variations of $(\chi_I)_{opt}$ with respect to X_{He}/X_{CO_2} and X_{H_2O}/X_{CO_2}. It is observed that, in general, variations in both CO_2 and H_2O contents strongly affect $(\chi_I)_{opt}$ in system 2, while variation in CO_2 content alone does so in system 1.

With the known optimum values of G_0 and χ_I the optimum operating conditions like p_0' and T_0' can be readily estimated, since χ_I, as given by (17), is a function of p_0', T_0' and the shape factor L'. However, since L' itself is a function of both the nozzle throat height and the expansion angle of the nozzle, $p_0'L'$ is directly computed as a function of T_0'. $p_0'L'$ is the binary scaling parameter (Anderson 1976) which would have more flexibility in estimating the reservoir pressure for any desired value of L'.

To estimate the appropriate optimum area ratio to be used corresponding to the optimum value of $p_0'L'$ the following procedure is adopted. First, for the given laser mixture and for the graphically known optimum value of χ_I, equations (1) to (4) are solved to obtain the optimum value of G_0 and also the value of ξ (to be designated ξ_{opt}) at which it occurs. $(G_0)_{opt}$ values can also be read-off from the graphs presented in figures 10 and 11. It can be shown (Reddy and Shanmugasundaram 1979a) that the optimum area ratio A_{opt} and ξ_{opt} are related by the following expression:

For He catalyst

$$[1{\cdot}165 - 0{\cdot}560\,(0{\cdot}1 + \log_{10} A_{opt})^{-0{\cdot}2}]\, A_{opt} = (k_1^{3{\cdot}37}\, k_2) \exp\,(S_0 - \xi_{opt}), \tag{25}$$

and for H_2O catalyst

$$[0{\cdot}669 - 0{\cdot}216\,(0{\cdot}194 + \log_{10} A_{opt})^{-0{\cdot}467}]\,A_{opt} = (k_1^{3{\cdot}98}\,k_2)\exp(S_0 - \xi_{opt}), \tag{26}$$

where k_1, k_2 and s_0 are functions of only T_0'. Hence, for the known value of ξ_{opt}, either (25) or (26) can be solved for A_{opt} as a function of T_0'.

Optimum values thus obtained for $p_0'L'$ and A have been plotted against T_0' in figures 12 to 24 for various mixture compositions for both systems 1 and 2. These figures show that, for any given gas composition, both $p_0'L'$ (therefore p_0' for a particular value of L') and A increases monotonically with T_0'. They also reveal a striking difference between systems 1 (He catalyst) and 2 (H_2O catalyst) namely, for the same order of optimum G_0 values, the optimum value of A is, in general, an order of magnitude larger in system 2 than that in system 1 and $p_0'L'$ values are of the same order in both the systems. This implies that system 2 is operationally superior to system 1. The data presented in figures 12 through 24 may appear numerous but these data are not repetitive in nature and useful in obtaining the optimum values of G_0 for a given laser composition; hence avoiding numerical computations.

Finally, it is to be pointed out that for the very large values ($\sim 10^3$) of A_{opt} obtained in some of the cases, the pressure levels in the nozzle are likely to be very low (approximately a few torr) with the result that Doppler line broadening might dominate or become comparable to collisional (Lorentz) line broadening. This aspect is being taken up by the authors as a next step. At very low gas densities, rapid intra-mode coupling of vibrational states, fundamental to the two-mode model of Anderson, might be lost. Under such circumstances a much more detailed analysis of the molecular kinetics would need to be invoked. If very low translational temperatures are

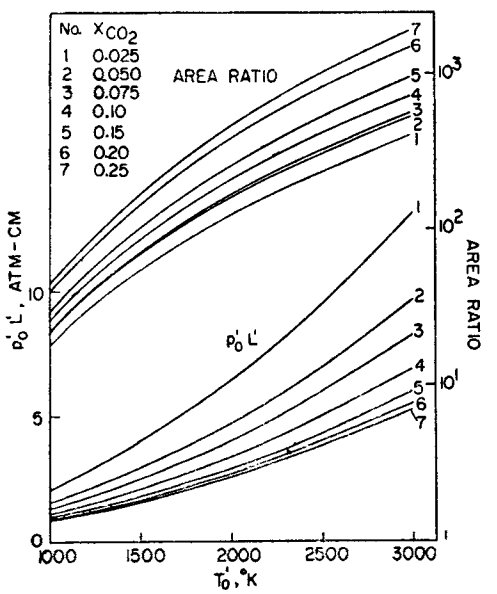

Figure 12

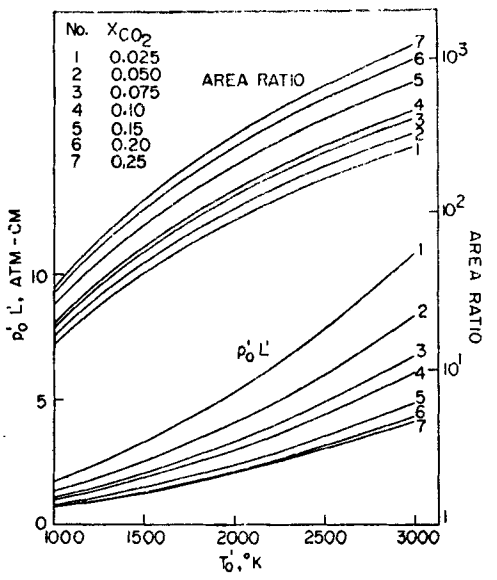

Figure 13

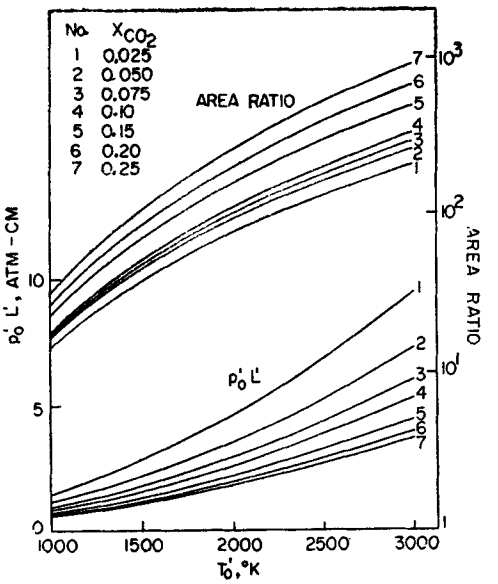

Figure 14

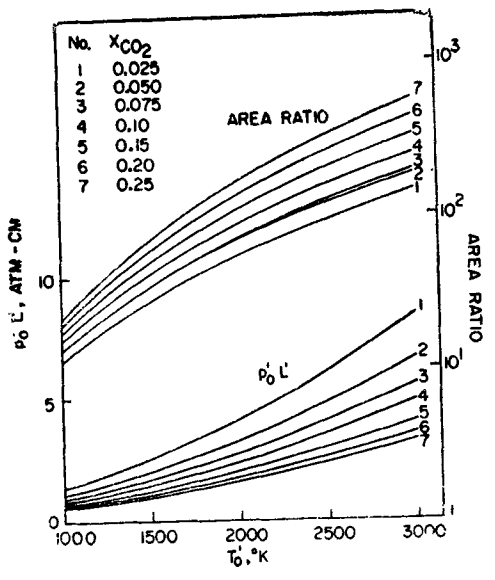

Figure 15

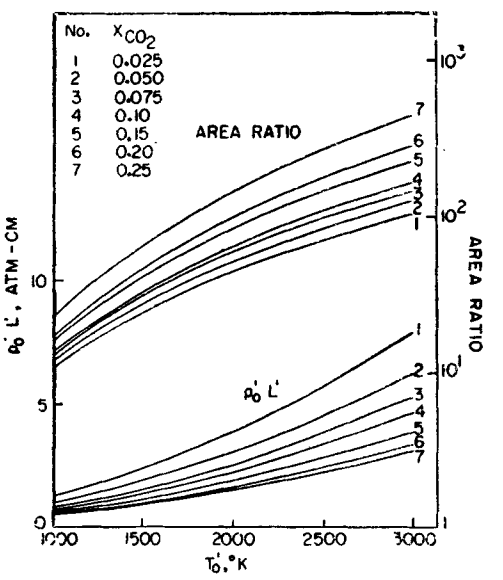

Figure 16

Figures 12–16. Variation of optimum area ratio and $p_0'L'$ with reservoir temperature and $ij = 1$ in system 1. **12.** $X_{He} = 0{\cdot}2$. **13.** $X_{He} = 0{\cdot}3$. **14.** $X_{He} = 0{\cdot}4$. **15.** $X_{He} = 0{\cdot}5$. **16.** $X_{He} = 0{\cdot}6$.

obtained at large expansion area ratios (A), as would be a reasonable expectation, additional concerns arise: (i) inadequate vibrational-relaxation kinetic data exist to support the extrapolation of the simplified τp correlations (see Appendix A of Reddy and Shanmugasundaram 1979a) to very low gas temperatures and (ii) maximum small-signal gain would be expected to shift far away from $P(20)$ to much lower-p-branch transitions, as dictated by the Botlzmann distribution of the rotational-state populations.

Lastly, it is worth noting here that only in the case of wedge nozzles with $ij=1$ equation (17) becomes independent of reservoir entropy S_0. Then, the universal correlating parameter χ_I depends only on the tertiary scaling parameter $(p_0' L'/T_0'^{3/2})$, which can be used to correlate the frozen vibrational temperatures in the nozzle flow calculations; this would be very useful for correlating the measured values.

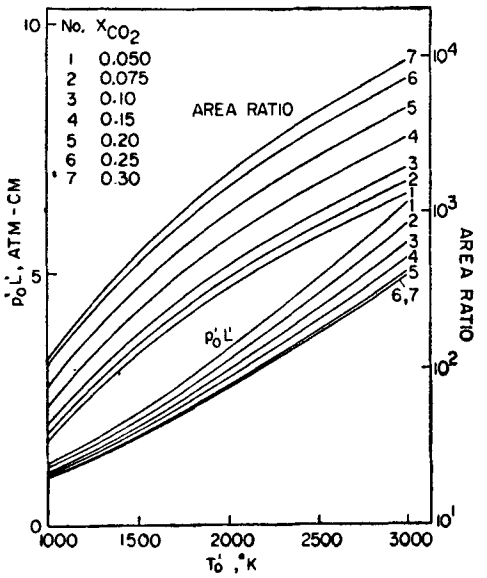

Figure 17

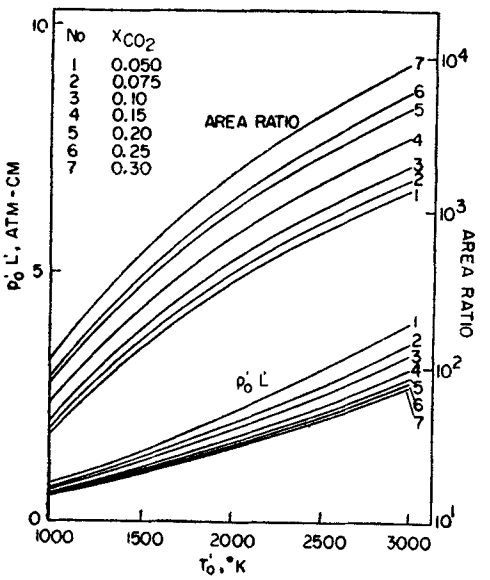

Figure 18

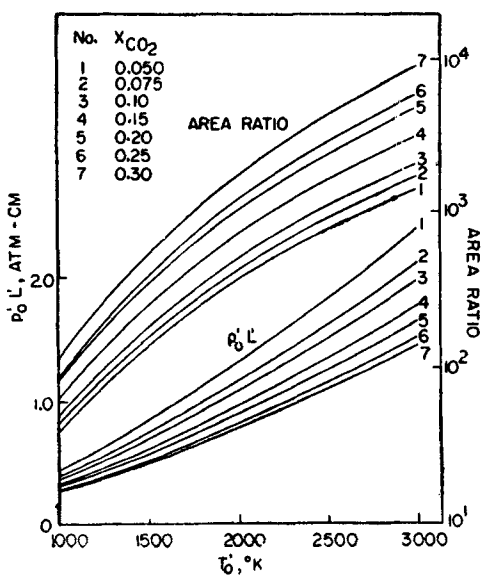

Figure 19

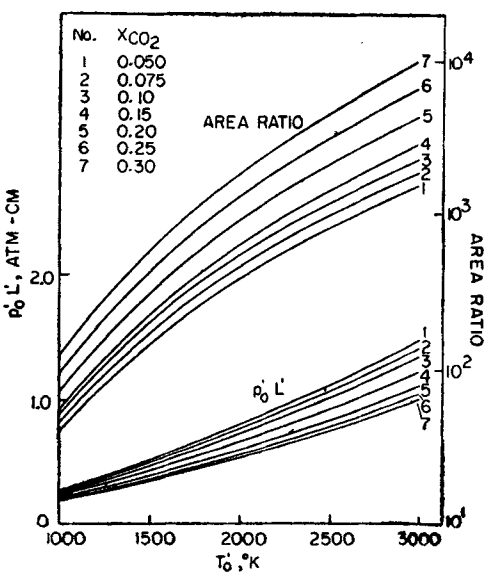

Figure 20

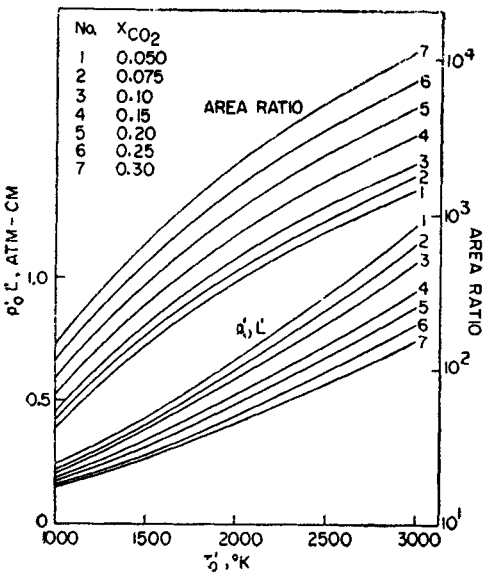

Figure 21

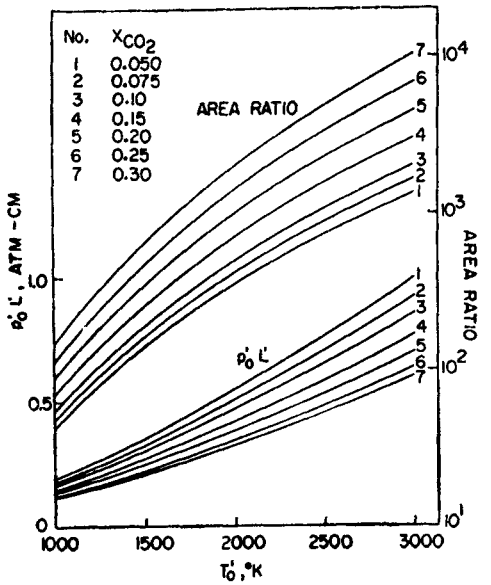

Figure 22

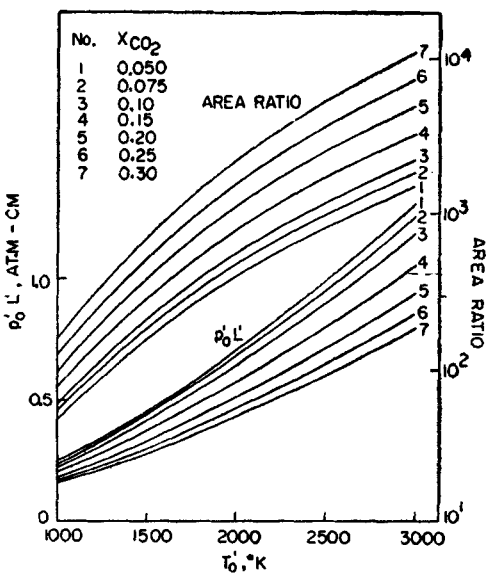

Figure 23

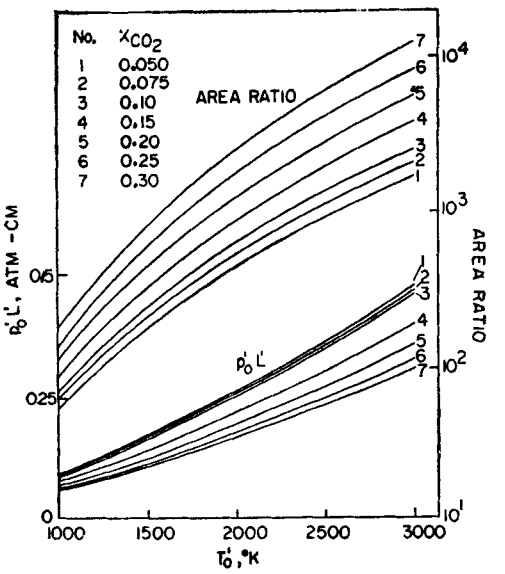

Figure 24

Figures 17–24. Variation of optimum area ratio and $p_0'L'$ with reservoir temperature and $ij = 1$ in system 2. **17.** $X_{H_2O} = 0{\cdot}01$. **18.** $X_{H_2O} = 0{\cdot}02$. **19.** $X_{H_2O} = 0{\cdot}04$. **20.** $X_{H_2O} = 0{\cdot}06$. **21.** $X_{H_2O} = 0{\cdot}08$. **22.** $X_{H_2O} = 0{\cdot}1$. **23.** $X_{H_2O} = 0{\cdot}15$. **24.** $X_{H_2O} = 0{\cdot}2$.

4. Conclusions

Based on the method given by Reddy and Shanmugasundaram (1979a), similar solutions have been obtained for the vibrational non-equilibrium flow along a family of GDL nozzles with $ij=1$, which represents a family of 2D wedge nozzles. From these

solutions optimum values of small-signal gain coefficient on the $P(20)$ vibrational-rotational transition in the 001→100 band of CO_2 and the corresponding values of the universal correlating parameter χ_I have been obtained and presented graphically for a wide range of laser mixture compositions for CO_2-N_2 systems, with either He or H_2O as the vibrational relaxation catalyst. From these results the optimum values for the area ratio and the binary scaling parameter, $p_0' L'$, as functions of reservoir temperature have been obtained and presented graphically for all the mixture compositions considered. Since L' is a function of the nozzle throat height and the expansion angle, the said $p_0' L'$ values can be used to estimate the optimum reservoir pressures for a wide range of nozzle sizes. The above results predict that small-signal optical-gains as high as $2/m$ on the 001→100 CO_2 transition can be obtained in CO_2-N_2-He systems with about 15 mole-% of CO_2 and about 40 mole-% of He; and G_0 as high as $3{\cdot}5/m$ in CO_2-N_2-H_2O systems with about 30 mole-% of CO_2 and 20 mole-% of H_2O. This analytical study further predicts that, in general, for the same order of optimum G_0 values, the optimum values of area ratio A is an order of magnitude larger in system 2 than in system 1 and $p_0' L'$ values are of the same order in both the systems. This implies that a system employing H_2O as a catalyst yields higher gain levels than that with He as a catalyst. Hence, the system 2 is operationally superior to system 1.

Acknowledgements

The help received by Dr K P J Reddy in preparing this paper is thankfully acknowledged. This research was supported by the Aeronautics Research and Development Board, Government of India.

References

Anderson Jr J D 1969 Naval Ordinance Lab. Report NOL TR-69-200 (unpublished)
Anderson Jr J D 1970 Naval Ordinance Lab. Report NOL TR-70-198 (unpublished)
Anderson Jr J D *et al* 1971 *Phys. Fluids* **14** 2620
Anderson Jr J D 1976 *Gasdynamic lasers. An Introduction* (New York: Academic Press) Chaps. IV and V
Christiansen W H, Russell D A and Hertzberg A 1975 *Fluid Mech.* **7** 115
Christiansen W H and Tsonges G A 1971 *Phys. Fluids* **14** 2011
Lordi J A, Mates R E and Moselle J R 1966 NASA Contractor Report CR-472 (unpublished)
Losev S A and Makarov V N 1975 *Sov. J. Quantum Electron.* **4** 905
McManus J I and Anderson Jr J D 1976 *AIAA J.* **14** 1770
Reddy N M and Shanmugasundaram V 1978 *Proc. Second Int. Symp. on Gasflow and Chemical Lasers, Brussels* (Washington: Hemisphere Publ., Corp.)
Reddy N M and Shanmugasundaram V 1979a *J. Appl. Phys.* **50** 2565
Reddy N M and Shanmugasundaram V 1979b *J. Appl. Phys.* **50** 2576